Poly (Vinyl Alcohol) Composite Membrane with Polyamidoamine Dendrimers for Efficient Separation of CO_2/H_2 and CO_2/N_2

yaxin zhao
Beijing Technology and Business University
Huafeng Tian (tianhuafeng@th.btbu.edu.cn)
Beijing Technology and Business University https://orcid.org/0000-0001-5123-3590
yuge ouyang
Beijing Technology and Business University
Aimin Xiang
Beijing Technology and Business University
Xiaogang Luo
Wuhan Institute of Technology
Xingwei Shi
Chinese Academy of Sciences

Research Article

Keywords: PVA, PAMAM, carrier, crystallinity, CO2 separation

Posted Date: October 28th, 2021

DOI: https://doi.org/10.21203/rs.3.rs-949246/v1

Abstract

Although polyvinyl alcohol (PVA) membranes are commonly used for CO_2 separation, there is still large development space in mechanical properties and high selectivity of the gas separation process. In this study, the gas separation performance and mechanical properties of the (PVA/Cu^{2+}) substrate membranes were improved by introducing polyamidoamine (PAMAM). PAMAM had an important effect on the gas adsorption and separation performance of the membrane. In addition, the gas adsorption and separation properties of the PVA/Cu^{2+}/PAMAM membrane (PPCm) were analyzed and studied when the inlet gas pressure and the species of mixed gases were variable. The results showed that the crystallinity and mechanical properties of the membrane with the PAMAM had been significantly improved. Young's modulus of PPCm with 30% PAMAM was 132% higher than that of the PVA/Cu^{2+} composite membrane without PAMAM. In addition, efficient separation efficiency and high selectivity of the gas separation process were observed. The separation factors of the PPCm for CO_2/H_2 and CO_2/N_2 were about three times higher than that of the PVA/Cu^{2+} substrate membranes. These results suggested that the introduction of PAMAM was promising for CO_2 separation and permeation.

Introduction

With the increasingly severe climate change, the separation of carbon dioxide from its emission sources has attracted global attention. Efforts have been made to find economic separation techniques to capture and separate CO_2[1–5]. Many CO_2 capture technologies have been developed, among which membrane separation is one of the most effective technologies. Compared with the traditional method of solvent absorption, membrane separation technology has the advantages of low investment cost, compact structure and no secondary pollution[6–8]. Polyvinyl alcohol (PVA) membrane is generally used in the mixed gas separation, because it has the large amount of the hydroxyl groups on its surface, which is conducive to the formation of a large diffusion rate difference in the membrane[9–13]. Nevertheless, the separation efficiency and mechanical properties of the membrane are still poor, and it cannot be commercially applied. The in-depth study of PVA membranes found that some metal ions with PVA could form macromolecular complexes[14–19]. Therefore, the mechanical properties of the PVA based membrane were further improved by introducing Cu^{2+} into the PVA membrane[10]. But its gas separation efficiency still needs to be improved.

Besides, there is a constraint trade-off between permeability and selectivity of commonly used polymer membranes. Polymer membranes with high permeability are usually less selective[20–23]. The promotion transfer membrane is to introduce the carrier inside the membrane, which is connected to the base membrane in the form of covalent bond. And then to promote the transfer of the component by reversible interaction between the carrier and a specific gas component in the mixed gases to be separated. Moreover, it may be mentioned that the carrier in the membrane is connected to the substrate in the form of covalent bond, which effectively solves the immobilization problem of the carrier[24, 25].

Polyamidoamine (PAMAM) is one of the most widely studied and mature tree-like molecules. It has high branching degree, symmetrical radial structure, high group density of surface amine groups. PAMAM can provide a large number of primary and secondary amine reaction active points, and has good hydrodynamic properties, easy membrane formation, good compatibility with PVA and so on[26–28].

In this work, based on the high permeability and selectivity of CO_2, PAMAM was introduced into PVA/Cu^{2+} membranes to prepare the PVA/PAMAM/Cu^{2+} promoting transfer membrane (PPCm) for further exploration. PAMAM could provide a large number of reversible reaction points with carbon dioxide. It was found that without affecting the permeability, the selection of CO_2 was highly improved. It provided a solution for the membrane to weaken the constraint trade-off between permeability and selectivity of it.

1. Experiment

Materials

PVA (117) was purchased from Kuraray Co.Ltd. $CuSO_4 \cdot 5H_2O$ (Analytical Reagent) was from Beijing Sinopharm Chemical Reagent Co., Ltd. Polyethersulfone (PES005) was from Beijing Vontron Technology Co., Ltd. PAMAM (zero-generation) was self-made in laboratory.

Preparation of the PPCm

PVA aqueous solution with solid content of 5% was prepared. Then certain amount of PAMAM was added into PVA solution by stirring 4 hours at room temperature. Whereafter, 5% Cu^{2+} was added into PVA/PAMAM solution by stirring 2 hours at room temperature. Then the solution was allowed to stand for a period of time to remove the bubbles. The PVA/PAMAM/Cu^{2+} membrane-forming solution was poured horizontally into the glass mold to get the PVA/PAMAM/Cu^{2+} promoting transfer membrane (PPCm). Finally, the PPCm was dried at 60°C for 24 hours.

Characterization

The structure of the PPCm was determined by Fourier transform infrared spectrometer (FTIR). The infrared scanning test was carried out by potassium bromide pressing method and Nicolet iN10MX (Thermo Electron, US) infrared tester. The scanning range was 4000cm^{-1}-500 cm^{-1}.

The structure of dried PPCm was observed and photographed with scanning electron microscope (SEM) (Quanta FEG-250, FEI Nanoports, US) operating at an acceleration voltage of 10KV.

The dried samples were tested with Different Scanning Calorimety (DSC) (Q2500 TA Instruments) in the N_2 atmosphere. And the sample weight was about 5-10 mg.

The mechanical properties test, the splines were placed 24 hours before testing. And it tested by the tensile speed of 50 mm/min at room temperature. During the experiment, each group of samples was tested 5 times, and the average value was taken.

Gas permeability and separation performance test：Effective sample size: Φ97 mm, transmission area: 38.48 cm^2 and gas test pressure: 0.5 MPa for the single gases CO_2, N_2 and H_2. Effective transmission area: 19.26 cm^2 and gas test pressure: 0.1 MPa - 0.5 MPa for mixed gases CO_2/N_2 with a volume radio of 85/15 and CO_2/H_2 with a volume radio of 50/50. The adsorption separation chamber was sealed with a sealing ring to ensure that the gas on the permeation side did not diffuse with the air during the test.

2. Results And Discussion

Fig 1 illustrated the schematic for the preparation of the PVA/Cu^{2+}/PAMAM membranes (PPCm) and the process of gases separation. PAMAM has high concentrations of amine groups which can enable the membrane to increase the selectivity of CO_2. Therefore, PAMAM was introduced into the PVA/Cu^{2+} membranes. Cu^{2+} and PAMAM complexed with PVA polymer chains to form the PPCm with significantly enhanced mechanical properties and separation efficiency[11, 20-22]. Generally, small molecular gases such as CO_2, N_2 and H_2 permeated through the membrane by the physical solution-diffusion mechanism. However, when PAMAM was introduced into the membrane, the amine groups in PAMAM could react reversibly with CO_2, so as to promote the permeation and separation of CO_2.

Structure characterization

Fig 2 showed the FTIR spectra of PPCm with different PAMAM contents. For the PVA/Cu^{2+} base membranes without PAMAM, there was 3416cm^{-1} stretching vibration attributed to -OH, 2919 cm^{-1} stretching vibration attributed to -C-H, the stretching vibration of 1434cm^{-1} was H-C-H, 912cm^{-1} and 842 cm^{-1} belonged to the stretching vibration of C-O-H and C-C respectively. But for the PPCm two new absorption peaks position at 1645 cm^{-1} and 1565 cm^{-1} belonged to the stretching vibration of -C-O- and bending vibration of -N-H in PAMAM. With the increase of PAMAM, they shifted to 1655 cm^{-1} and 1555 cm^{-1}. At this time, the peak position of -OH gradually moved to a lower wave number. The shift of these functional group peaks was mainly due to the hydrogen bond interaction between the -NH-CO- group in the PAMAM and the -OH group in the PVA. The strong hydrogen bonding interaction could act as physical crosslinking agents, which would enhance the mechanical performances of the matrix.

Fig 2 showed the SEM images of PPCm with different PAMAM contents. The crosssection were smooth and glossy, and no PAMAM agglomeration was observed. It can be found that the surface roughness of PPCm increased with increasing of PAMAM contents, indicating the tough fracture. Therefore, the excellent compatibility between PAMAM and PVA/Cu^{2+} matrix can be concluded.

DSC analysis

Fig 3 showed the DSC curves and crystallinity of PPCm with different PAMAM contents. From the endothermic curves of the PPCm, PVA crystallization peak at ca. 180°C could be observed. With the introduction of PAMAM, the crystallization onset temperature and the crystallization peak temperature decreased with the increase of PAMAM. The crystallinity of PPCm could be calculated from the follows:

$$X_c = \frac{\Delta H_c}{f \times \Delta H_0} \times 100\%$$

ΔH_0 is the melting enthalpy of the PVA membrane at 100% crystallinity; the ΔH_c is the melting enthalpy of the transfer membrane; and the *f* is the mass fraction of the polymer matrix.

It could be concluded that the crystallinity of PPCm was obviously higher than that of PVA/Cu^{2+} based membrane without PAMAM, as shown in Fig 3 (c). With the increase of PAMAM, the crystallinity of PPCm increased obviously. The results showed that the PAMAM with high degree of branching exhibited heterogeneous nucleation effect in the PVA matrix, which could increase the crystallinity.

Mechanical properties

Fig 4 illustrated tensile strength, Young's modulus and elongation at break of the PPCm with different PAMAM contents. Fig 4 (a) showed that the tensile strength of 5% PAMAM increased to the maximum. And then the tensile strength of PPCm decreased continuously with the increase of PAMAM content. PAMAM exhibited reinforcing effect in the matrix, and increased the rigidity of the membrane. As shown in Fig 4 (b), with the increase of PAMAM, the Young's modulus of PPCm increased obviously. The Young's modulus of the transfer promoting membrane with the 30% PAMAM content increased by 132% compared with the PVA/Cu^{2+} base membrane without PAMAM. The fracture elongation of PPCm decreased significantly with the increase of PAMAM content, as shown in Fig 4(c). When the existence of PAMAM was too much, it destroyed the structure of the membrane, resulting in the decrease of tensile strength and elongation at break. Besides, the results of Young's modulus and tensile strength were mainly due to the increase of crystallinity of the PPCm, as well as the strong hydrogen bonding interactions. The raise of intermolecular force leaded to the promotion of Young's modulus and the decline of tensile strength.

Gas Separation Properties

Separation properties for a single gas

The gas permeation unit (GPU) of three single gases, CO_2, H_2 and N_2, were measured, as shown in the Fig 5. The CO_2 GPU of the PPCm increased with the increase of PAMAM. The gas permeation unit of CO_2 was as high as 120 GPU when the PAMAM concentration was 30%. It was much greater than that of N_2 and

H_2. Even with the increase of PAMAM concentration, the gas permeation unit slightly decreased. The gas permeation of N_2 and H_2 was independent of the PAMAM content. This was mainly due to the reduction of physical solution-diffusion in the process of gas permeation. However, in the course of CO_2 permeation through PPCm with amine carriers, there was not only physical solution-diffusion mechanism, but also facilitated transport mechanism. This fully illustrated that the introduction of PAMAM would have an efficient effect on the separation of mixed gases.

Separation properties of the mixed gas

As shown in Fig 6, the gas permeation unit of CO_2/N_2 with a volume ratio of 15/85 was measured under different inlet gas pressures. The GPU of CO_2 and N_2 increased significantly with the increase of PAMAM contents. And the CO_2 and N_2 permeation unit increased at higher inlet gas pressure. When the PAMAM was 10% and the inlet gas pressure was 0.5 MPa, the CO_2 permeation unit was 7.3 GPU and the N_2 permeation unit was 1.6 GPU, as illustrated in Fig 6 (a, b). Separation factor was an important parameter to measure the separation ability of membranes. The separation factors of the CO_2/N_2 of PPCm were calculated, as shown in Fig 6(c). As the PAMAM content increasing, the separation factor of CO_2/N_2 increased obviously. When the PAMAM was 10% and the inlet gas pressure was 0.5 MPa, the separation factor of the PPCm was 14.

The permeation of small molecular gases such as CO_2 and N_2 through the membrane was the physical-diffusion mechanism. Beyond that, there was another facilitated transport mechanism for CO_2 permeation through the PPCm. Therefore, the gas permeation unit of CO_2 was obviously larger than that of the N_2. And with the increase of PAMAM contents, the separation factor increased. Because it increased the density of effective amine groups which were capable of interacting with CO_2. The CO_2 and N_2 permeation unit increased at higher inlet gas pressure, because of the coupling of two gases in the mixture. In general, the separation factors of PPCm increased with the increase of PAMAM.

Under different inlet gas pressures, the gas permeation unit of CO_2/H_2 with a volume ratio of 50/50 was illustrated in Fig 7 (a, b). The CO_2 permeation unit generally decreased and then stabilized with the increase of PAMAM content, while the H_2 permeation unit generally decreased with the increase of PAMAM content. The CO_2/H_2 separation factors of the PVA/PAMAM/Cu^{2+} transfer membranes were calculated, as shown in Fig 7 (c). And when the PAMAM was 20% and the inlet gas pressure was 0.5 MPa, the separation factor of the PPCm was 1.3, reaching the maximum. The separation factor of CO_2/H_2 increased steadily, with the increase of PAMAM contents. When the PAMAM content exceeded 20%, the separation factor of PPCm for CO_2/H_2 decreased.

The small size of H_2 gas molecules were easier to permeate through the membrane than CO_2 and N_2 molecules by the dissolution-diffusion mechanism. When the PAMAM content increased, the tightness of the membrane increased, resulting in the decline of H_2 permeation unit. However, CO_2 mainly permeated through the PPCm by the facilitated transport mechanism. Therefore, the separation factor of the PPCm of the CO_2/H_2 was much smaller than that of CO_2/N_2. When the PAMAM content was too much, the effective amine density decreased. And it had resulted in the decline of the separation factors.

4. Conclusion

In this study, PAMAM was successfully introduced into the PVA/Cu^{2+} base membrane, and the uniformly transparent PPCm was successfully prepared. PAMAM could act as heterogeneous nucleation agents in the PVA/Cu^{2+} base membrane to improve the crystalstallization of the transfer membrane. The introduction of the mechanical properties of PAMAM reduced the fracture elongation and increased the elastic modulus. The introduction of PAMAM has little effect on the gas permeation unit (GPU) of N_2 and H_2. But it significantly improved the GPU of CO_2. As the content of PAMAM increased, the separation factor of PPCm of CO_2/N_2 and CO_2/H_2 were increased. The separation factor of PPCm of CO_2/N_2 was much larger than that of CO_2/H_2. This membrane can be used for CO_2 capture and separation, and it will make an important contribution to the greenhouse effect.

Declarations

Acknowledgement

This work was supported by Beijing Natural Science Foundation (2202014), School Level Cultivation Fund of Beijing Technology and Business University for Distinguished and Excellent Young Scholars (BTBUYP2021), funding of Hubei key Laboratory of Novel Reactor and Green Chemical Technology (Wuhan Institute of Technology).

References

1. Torstensen, J. Ø.; Helberg, R. M. L.; Deng, L.; Gregersen, Ø. W.; Syverud, K., PVA/nanocellulose nanocomposite membranes for CO2 separation from flue gas (2019) *International Journal of Greenhouse Gas Control 81*, 93-102.doi:10.1016/j.ijggc.2018.10.007
2. Maheswari, A. U.; Palanivelu, K., Separation of carbon dioxide and nitrogen gases using novel composite membranes (2017) *Canadian Journal of Chemistry 95* (1), 57-67.doi:10.1139/cjc-2016-0090
3. Iyer, G. M.; Liu, L.; Zhang, C., Hydrocarbon separations by glassy polymer membranes (2020) *Journal of Polymer Science 58* (18), 2482-2517.doi:10.1002/pol.20200128
4. Francisco, G. J.; Chakma, A.; Feng, X., Membranes comprising of alkanolamines incorporated into poly(vinyl alcohol) matrix for CO2/N2 separation (2007) *Journal of Membrane Science 303* (1-2), 54-63.doi:10.1016/j.memsci.2007.06.065
5. Wang, Z.; Pan, Z., Preparation of hierarchical structured nano-sized/porous poly(lactic acid) composite fibrous membranes for air filtration (2015) *Applied Surface Science 356*, 1168-

1179.doi:10.1016/j.apsusc.2015.08.211

6. Liu, H.; Liang, X., Strategy for promoting low-carbon technology transfer to developing countries: The case of CCS (2011) *Energy Policy 39* (6), 3106-3116.doi:10.1016/j.enpol.2011.02.051
7. Taniguchi, I.; Kinugasa, K.; Toyoda, M.; Minezaki, K., Effect of amine structure on CO2 capture by polymeric membranes (2017) *Sci Technol Adv Mater 18* (1), 950-958.doi:10.1080/14686996.2017.1399045
8. Mondal, A.; Barooah, M.; Mandal, B., Effect of single and blended amine carriers on CO 2 separation from CO 2 /N 2 mixtures using crosslinked thin-film poly(vinyl alcohol) composite membrane (2015) *International Journal of Greenhouse Gas Control 39*, 27-38.doi:10.1016/j.ijggc.2015.05.002
9. Shirvani, H.; Sadeghi, M.; Taheri Afarani, H.; Bagheri, R., Polyurethane/Poly(vinyl alcohol) Blend Membranes for Gas Separation (2018) *Fibers and Polymers 19* (5), 1119-1127.doi:10.1007/s12221-018-1023-6
10. Liu, Q.; Ge, X.; Xiang, A.; Tian, H., Effect of copper sulfate pentahydrate on the structure and properties of poly(vinyl alcohol)/graphene oxide composite films (2016) *Journal of Applied Polymer Science 133* (46).doi:10.1002/app.44135
11. Kim, D. H.; Park, M. S.; Kim, N. U.; Ryu, D. Y.; Kim, J. H., Multifunctional Amine-Containing PVA-g-POEM Graft Copolymer Membranes for CO2 Capture (2018) *Macromolecules 51* (15), 5646-5655.doi:10.1021/acs.macromol.8b01198
12. Lilleby Helberg, R. M.; Dai, Z.; Ansaloni, L.; Deng, L., PVA/PVP blend polymer matrix for hosting carriers in facilitated transport membranes: Synergistic enhancement of CO2 separation performance (2020) *Green Energy & Environment 5* (1), 59-68.doi:10.1016/j.gee.2019.10.001
13. Jahan, Z.; Niazi, M. B. K.; Hägg, M.-B.; Gregersen, Ø. W., Cellulose nanocrystal/PVA nanocomposite membranes for CO2/CH4 separation at high pressure (2018) *Journal of Membrane Science 554*, 275-281.doi:10.1016/j.memsci.2018.02.061
14. Edubilli, S.; Gumma, S., A systematic evaluation of UiO-66 metal organic framework for CO2/N2 separation (2019) *Separation and Purification Technology 224*, 85-94.doi:10.1016/j.seppur.2019.04.081
15. Shakeel, I.; Hussain, A.; Farrukh, S., Effect Analysis of Nickel Ferrite (NiFe2O4) and Titanium Dioxide (TiO2) Nanoparticles on CH4/CO2 Gas Permeation Properties of Cellulose Acetate Based Mixed Matrix Membranes (2019) *Journal of Polymers and the Environment 27* (7), 1449-1464.doi:10.1007/s10924-019-01442-x
16. Deeksha, B.; Sadanand, V.; Hariram, N.; Rajulu, A. V., Preparation and properties of cellulose nanocomposite fabrics with in situ generated silver nanoparticles by bioreduction method (2021) *Journal of Bioresources and Bioproducts 6* (1), 75-81.doi:10.1016/j.jobab.2021.01.003
17. Barooah, M.; Mandal, B., Synthesis, characterization and CO2 separation performance of novel PVA/PG/ZIF-8 mixed matrix membrane (2019) *Journal of Membrane Science 572*, 198-209.doi:10.1016/j.memsci.2018.11.001

18. Niazi, M. B. K.; Jahan, Z.; Ahmed, A.; Rafiq, S.; Jamil, F.; Gregersen, Ø. W., Effect of Zn-Cyclen Mimic Enzyme on Mechanical, Thermal and Swelling Properties of Cellulose Nanocrystals/PVA Nanocomposite Membranes (2020) *Journal of Polymers and the Environment 28* (7), 1921-1933.doi:10.1007/s10924-020-01737-4
19. Ashok, B.; Hariram, N.; Siengchin, S.; Rajulu, A. V., Modification of tamarind fruit shell powder with in situ generated copper nanoparticles by single step hydrothermal method (2020) *Journal of Bioresources and Bioproducts 5* (3), 180-185.doi:10.1016/j.jobab.2020.07.003
20. Chowdhury, F. A.; Yamada, H.; Higashii, T.; Goto, K.; Onoda, M., CO2 Capture by Tertiary Amine Absorbents: A Performance Comparison Study (2013) *Industrial & Engineering Chemistry Research 52* (24), 8323-8331.doi:10.1021/ie400825u
21. Fadhel, B.; Hearn, M.; Chaffee, A., CO2 adsorption by PAMAM dendrimers: Significant effect of impregnation into SBA-15 (2009) *Microporous and Mesoporous Materials 123* (1-3), 140-149.doi:10.1016/j.micromeso.2009.03.040
22. Dutcher, B.; Fan, M.; Russell, A. G., Amine-based CO2 capture technology development from the beginning of 2013-a review (2015) *ACS Appl Mater Interfaces 7* (4), 2137-48.doi:10.1021/am507465f
23. Barooah, M.; Mandal, B., Enhanced CO2 separation performance by PVA/PEG/silica mixed matrix membrane (2018) *Journal of Applied Polymer Science 135* (28).doi:10.1002/app.46481
24. Gong, P.; Zhao, Y.; Li, K.; Tian, H.; Li, C., Effect of Plasticizer Content on the Structure and Properties of SPI/MA-g-PBAT Blend Films (2021) *Journal of Polymers and the Environment*.doi:10.1007/s10924-021-02223-1
25. Li, K.; Fan, G.; Tian, H.; Yuan, L.; Yao, Y.; Xiang, A.; Luo, X., Highly Oriented Thermoplastic Poly (vinyl alcohol) Films by Uniaxial Drawing: Effect of Stretching Temperature and Draw Ratio (2021) *Journal of Polymers and the Environment 29* (10), 3263-3270.doi:10.1007/s10924-021-02113-6
26. Wang, X.; Chen, H.; Zhang, L.; Yu, R.; Qu, R.; Yang, L., Effects of coexistent gaseous components and fine particles in the flue gas on CO 2 separation by flat-sheet polysulfone membranes (2014) *Journal of Membrane Science 470*, 237-245.doi:10.1016/j.memsci.2014.07.040
27. Niazi, M. B. K.; Jahan, Z.; Berg, S. S.; Gregersen, O. W., Mechanical, thermal and swelling properties of phosphorylated nanocellulose fibrils/PVA nanocomposite membranes (2017) *Carbohydr Polym 177*, 258-268.doi:10.1016/j.carbpol.2017.08.125
28. Klepić, M.; Setničková, K.; Lanč, M.; Žák, M.; Izák, P.; Dendisová, M.; Fuoco, A.; Jansen, J. C.; Friess, K., Permeation and sorption properties of CO2-selective blend membranes based on polyvinyl alcohol (PVA) and 1-ethyl-3-methylimidazolium dicyanamide ([EMIM][DCA]) ionic liquid for effective CO2/H2 separation (2020) *Journal of Membrane Science 597*.doi:10.1016/j.memsci.2019.117623

Figures

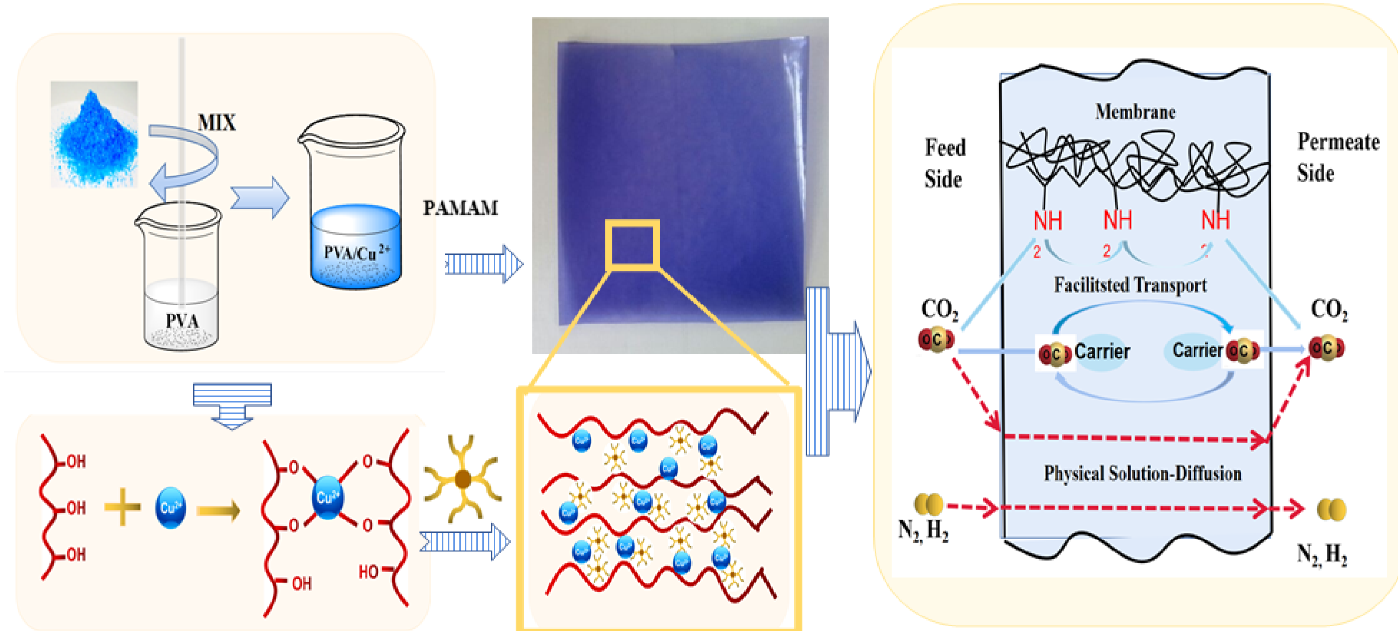

Figure 1

the schematic for preparation of the PPCm and the process of gases separation

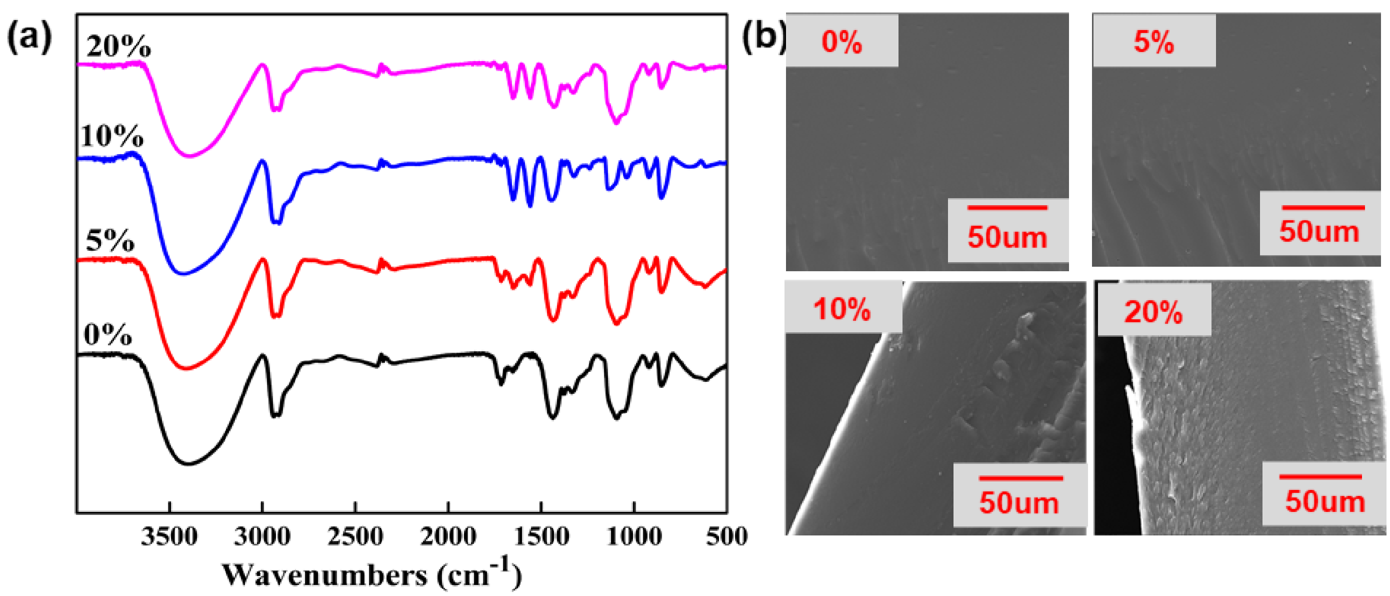

Figure 2

(a) the FTIR spectra and (b)the SEM images of PPCm with different PAMAM contents

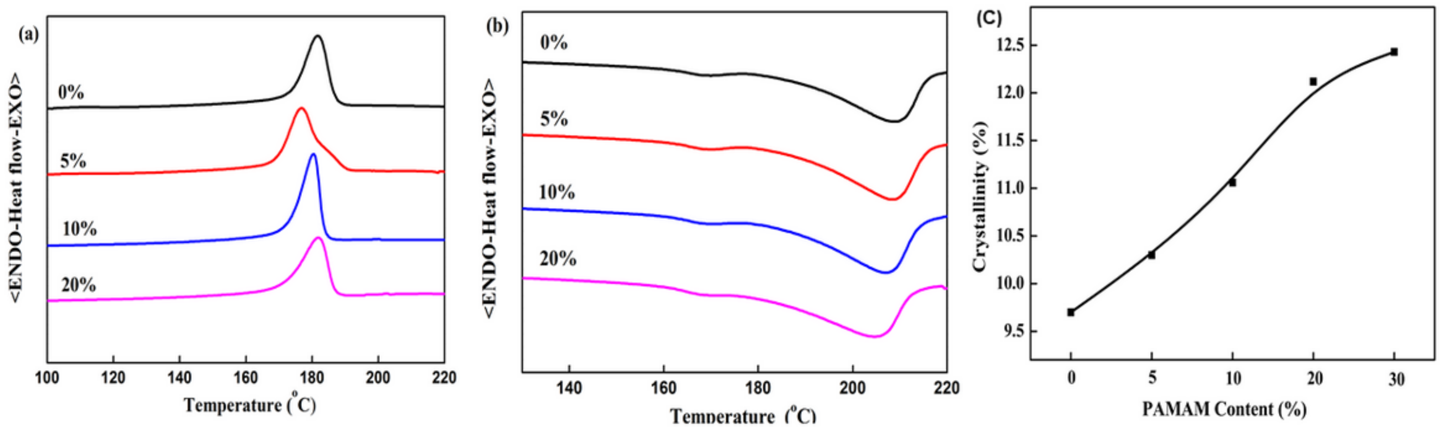

Figure 3

DSC (a) heating curves (b) cooling curves and (c) Crystallinity of PPCm with different PAMAM contents

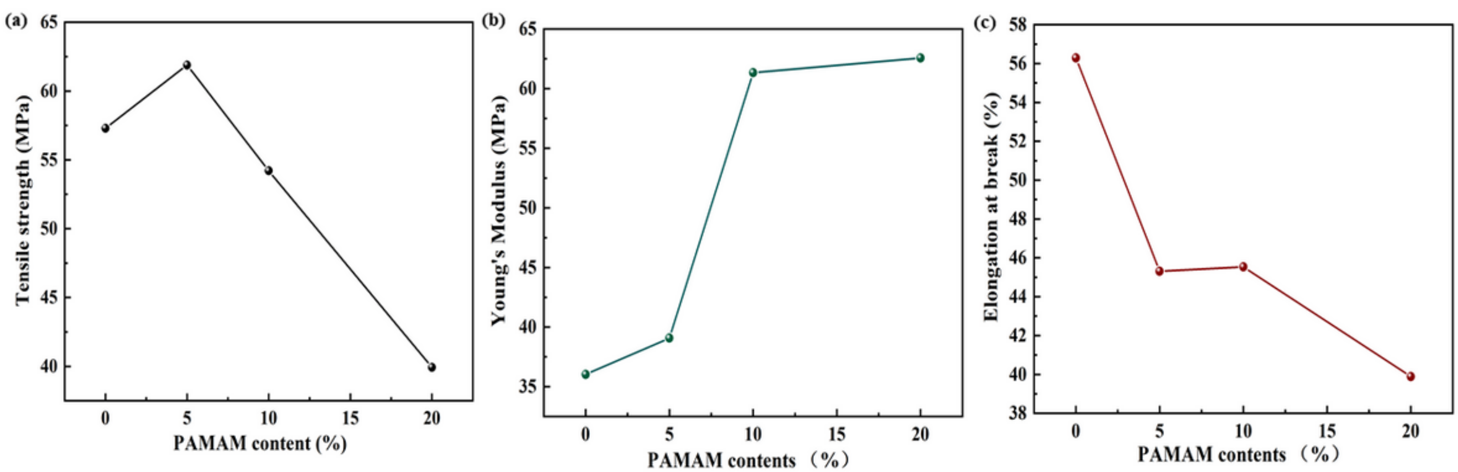

Figure 4

(a) Tensile strength (b) Young’s Modulus and (c) Elongation at break of the PPCm with different PAMAM contents

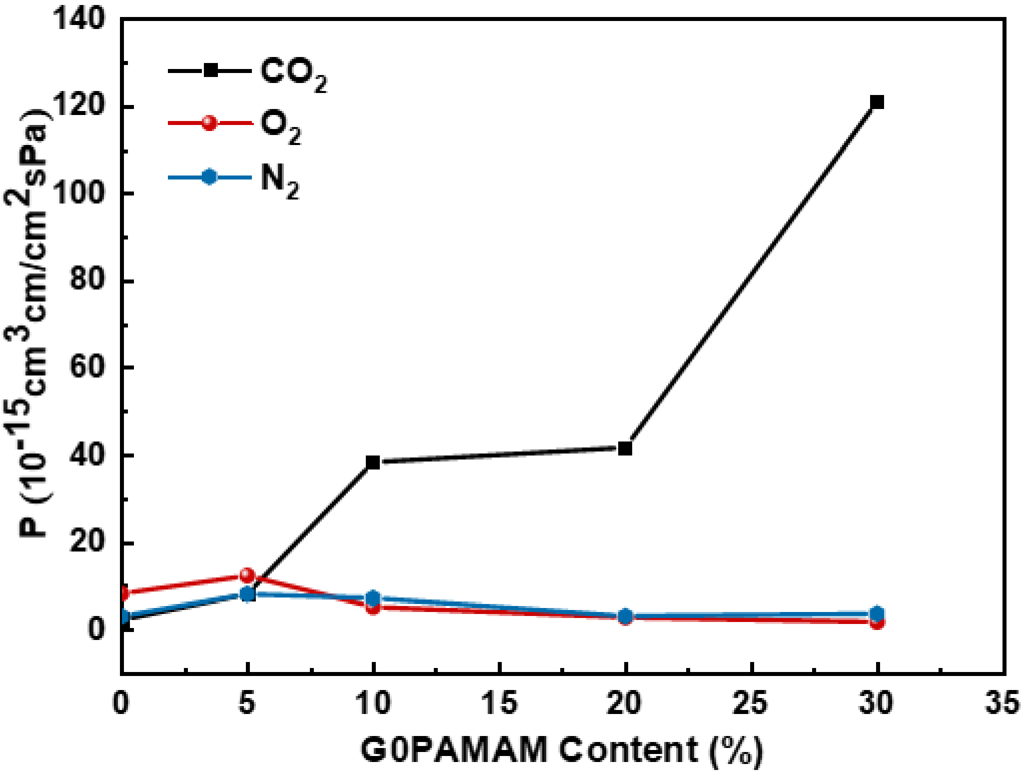

Figure 5

The gas permeation unit of the PPCms with different PAMAM contents

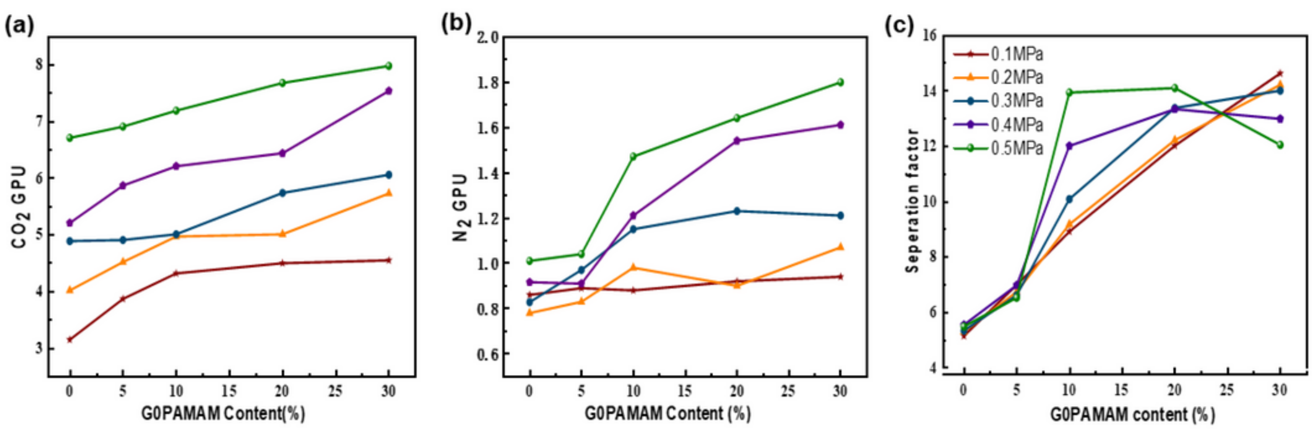

Figure 6

The gas permeation unit and the separation factors of the CO2 /N2 with different PAMAM contents

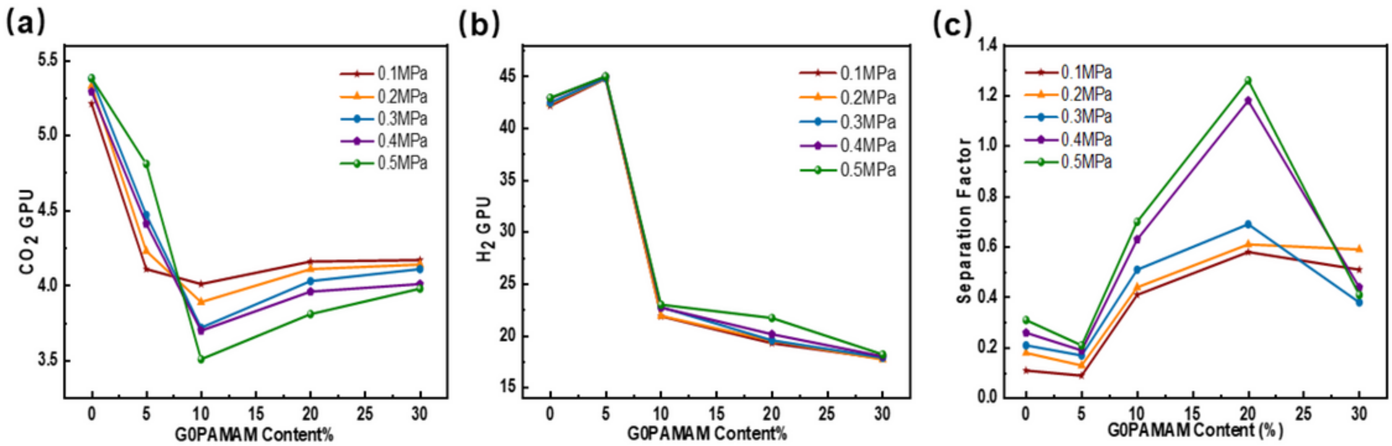

Figure 7

The gas permeation unit and the separation factors of the CO2 /H2 with different PAMAM content